

Error Probability and SINR Analysis of Optimum Combining in Rician Fading

Matthew R. McKay[†], Alberto Zanella[‡], Iain B. Collings^{*}, Marco Chiani[‡]

[†]Dept. of Electronic and Computer Engineering, Hong Kong University of Science and Technology, Hong Kong

[‡]IEIIT-BO/CNR, DEIS, University of Bologna, Bologna, Italy

^{*}Wireless Technologies Laboratory, ICT Centre, CSIRO, Sydney, Australia

Abstract

This paper considers the analysis of optimum combining systems in the presence of both co-channel interference and thermal noise. We address the cases where either the desired-user or the interferers undergo Rician fading. Exact expressions are derived for the moment generating function of the SINR which apply for arbitrary numbers of antennas and interferers. Based on these, we obtain expressions for the symbol error probability with M -PSK. For the case where the desired-user undergoes Rician fading, we also derive exact closed-form expressions for the moments of the SINR. We show that these moments are directly related to the corresponding moments of a Rayleigh system via a simple scaling parameter, which is investigated in detail. Numerical results are presented to validate the analysis, and to examine the impact of Rician fading on performance.

I. INTRODUCTION

Adaptive antenna arrays with linear diversity combining provide an effective means of increasing the performance of wireless communications systems. Of the various combining strategies which have been proposed, optimum combining (OC) [1] is the most effective solution for multi-user systems which operate in the presence of both co-channel interference and thermal noise. These systems are designed to exploit channel knowledge at the receiver to maximize the signal-to-interference-plus-noise ratio (SINR) for every channel use.

For OC systems where both the desired-user and interferer channels undergo Rayleigh fading, the performance has been well-studied [2–16]; with results now available for the symbol (and bit) error probability, the SINR distribution, and the outage probability. In practical scenarios however, the channels often include line-of-sight (LoS) paths, in which case Rician fading is appropriate. Prominent examples supported by physical measurements, include microcellular mobile and indoor radio applications [18]. Rician paths are also expected to arise in ad-hoc networking applications (especially for dense networks), which are currently receiving considerable interest.

However, despite their practical significance, and in contrast to the Rayleigh fading case, there are currently very few OC performance results which apply for Rician fading, and none which consider error probability. The few results which do apply for these channels are presented in [14, 18–20], all of which focus on characterizing the SINR probability density function (p.d.f.) or outage probability, and restrict attention to interference-limited scenarios. For these scenarios, the thermal noise is neglected, and the number of interferers is restricted to be greater than or equal to the number of antenna elements. This simplifies the analysis since the resulting signal-to-interference-ratio (SIR) follows a noncentral multivariate F distribution, thereby allowing classical multivariate statistics results from [21] to be directly leveraged.

In this paper we analyze the error probability of OC systems in Rician fading. We consider the general practical scenario where the received signals are subject to both co-channel interference and thermal noise. Our results allow for arbitrary numbers of interferers and receive antennas. We consider two particular cases: one where the desired-user is subject to Rician fading and the interferers undergo Rayleigh fading (denoted Rician-Rayleigh); and one where the desired user is subject to Rayleigh fading and the interferers undergo Rician fading (denoted Rayleigh-Rician). The analysis differs significantly from the interference-limited cases in [14, 18–20], since existing

results from classical multivariate statistics cannot be directly applied.

We make the following key contributions:

- A new accurate approximation is presented for the symbol error probability (SEP) of OC with coherent M -PSK modulation. This approximation is a closed-form expression in terms of the moment generating function (m.g.f.) of the SINR.
- Exact expressions are derived for the m.g.f. of the SINR of Rician-Rayleigh and Rayleigh-Rician OC systems. These expressions apply for arbitrary numbers of antennas and interferers, and permit fast efficient evaluation of the exact and approximate SEP.
- Exact closed-form expressions are presented for the moments of the SINR for the case of Rician-Rayleigh fading. Remarkably, we find that all of the moments in this case are directly related to the corresponding moments of a Rayleigh-Rayleigh system via a simple scaling parameter; which we investigate in detail.
- New simple closed-form expressions are given for the SINR m.g.f. and moments for the special case of Rayleigh-Rayleigh fading.

Numerical results are presented to validate the analysis, and to examine the impact of Rician fading on performance. These show that for the Rician-Rayleigh case, the performance improves as the Rician fading becomes more dominant, whereas for the Rayleigh-Rician case the Rician component may improve or degrade performance, depending on the geometry of the interferer Rician paths.

II. SYSTEM DESCRIPTION

We consider a multi-user system where the receiver of interest optimally-combines the output from N_A receive antennas. The desired signal is corrupted by N_I interferers and thermal noise. After matched filtering and sampling at the symbol rate, the array output vector at time k can be written as [7]:

$$\mathbf{z}(k) = \sqrt{E_D} \mathbf{c}_D b_0(k) + \mathbf{z}_{\text{IN}}(k), \quad (1)$$

with the interference plus noise term

$$\mathbf{z}_{\text{IN}}(k) = \sum_{j=1}^{N_I} \sqrt{E_I} \mathbf{c}_{\text{I},j} b_j(k) + \mathbf{n}(k), \quad (2)$$

where E_D and E_I are the mean (over fading) energies of the desired and interfering signals, respectively; $\mathbf{c}_D = [c_{D,1}, \dots, c_{D,N_A}]^T$ and $\mathbf{c}_{\text{I},j} = [c_{\text{I},j,1}, \dots, c_{\text{I},j,N_A}]^T$ are the desired and j^{th} interference

normalized propagation vectors, respectively; $b_0(k)$ and $b_j(k)$ are the desired and interfering data samples, respectively, and $\mathbf{n}(k)$ represents the additive noise.

We model \mathbf{c}_D and $\mathbf{c}_{I,j}$ as uncorrelated complex Gaussian vectors with possibly non-zero means (in particular we are interested in Rician fading in this paper); $b_j(k)$ are modeled as uncorrelated zero-mean random variables; and without loss of generality, $b_0(k)$ and $b_j(k)$ are assumed to have unit variance. The additive noise is modeled as a zero-mean white Gaussian random vector with $\mathbb{E} [\mathbf{n}(k)\mathbf{n}^\dagger(k)] = N_0\mathbf{I}_{N_A}$.

Note that here we make the common assumption (eg. as in [7, 11–13], among others) that the interferers have equal-power. For the special case of Rayleigh fading, the performance with unequal-power interferers has been investigated in [16], however for Rician fading it still remains an open problem.

The SINR at the output of the OC is given by [1]

$$\gamma = E_D \mathbf{c}_D^\dagger \mathbf{R}^{-1} \mathbf{c}_D, \quad (3)$$

where \mathbf{R} denotes the short-term covariance matrix of $\mathbf{z}_{IN}(k)$, conditioned on all interference propagation vectors, as follows

$$\mathbf{R} = N_0 \mathbf{I}_{N_A} + E_I \mathbf{C}_I \mathbf{C}_I^\dagger \quad (4)$$

where $\mathbf{C}_I = [\mathbf{c}_{I,1}, \mathbf{c}_{I,2}, \dots, \mathbf{c}_{I,N_I}]$. It is important to remark that \mathbf{R} and, consequently γ , vary at the fading rate, which is assumed to be much slower than the symbol rate.

III. SYMBOL ERROR PROBABILITY

In this paper we employ moment generating function (m.g.f.) based approaches to derive new exact and approximate symbol error probability expressions for OC systems in Rician fading. Note that m.g.f.-based techniques have also been previously used for the analysis of OC systems in Rayleigh fading (eg. see [6, 11]).

A. Exact SEP

Here we present expressions for M -PSK. Similar expressions can be generated for M -QAM.

Using a standard approach [22], the SEP with coherent M -PSK can be expressed as

$$P_e = \frac{1}{\pi} \int_0^\Theta M_\gamma \left(-\frac{c_{\text{MPSK}}}{\sin^2 \theta} \right) d\theta \quad (5)$$

where $\Theta \triangleq \pi(M-1)/M$, $c_{\text{MPSK}} \triangleq \sin^2(\pi/M)$, and $M_\gamma(\cdot)$ is the moment generating function (m.g.f.) of the SINR γ given by

$$M_\gamma(s) = \mathbb{E}_\gamma [e^{s\gamma}] . \quad (6)$$

Note that for OC, from (3), the expectation in (6) involves averaging over both the distribution of the user channel vector \mathbf{c}_D and the interference channel matrix \mathbf{C}_I .

B. Approximate SEP

Here we present a new approximation to (5) which does not require integration over θ . We start by using (5) and (6) to write

$$P_e = \mathbb{E}_\gamma \left[\frac{1}{\pi} \int_0^{\frac{\pi}{2}} \exp\left(-\frac{c_{\text{MPSK}}\gamma}{\sin^2\theta}\right) d\theta + \frac{1}{\pi} \int_{\frac{\pi}{2}}^\Theta \exp\left(-\frac{c_{\text{MPSK}}\gamma}{\sin^2\theta}\right) d\theta \right] . \quad (7)$$

Now, using [23, eq. (3)] and [23, eq. (14)] we can approximate the left-hand integral as

$$\frac{1}{\pi} \int_0^{\frac{\pi}{2}} \exp\left(-\frac{c_{\text{MPSK}}\gamma}{\sin^2\theta}\right) d\theta \approx \frac{1}{12} e^{-c_{\text{MPSK}}\gamma} + \frac{1}{4} e^{-4c_{\text{MPSK}}\gamma/3} . \quad (8)$$

The right-hand integral can also be well approximated by the area of a trapezoid with parallel sides of length $e^{-c_{\text{MPSK}}\gamma}$ and $e^{-c_{\text{MPSK}}\gamma/\sin^2(\Theta)}$ and height $\Theta - \pi/2$; i.e.

$$\frac{1}{\pi} \int_{\pi/2}^\Theta \exp\left(-\frac{c_{\text{MPSK}}\gamma}{\sin^2\theta}\right) d\theta \approx \frac{1}{2\pi} \left(e^{-c_{\text{MPSK}}\gamma} + e^{-c_{\text{MPSK}}\gamma/\sin^2\Theta} \right) (\Theta - \pi/2) . \quad (9)$$

Now substituting (9) and (8) into (7), we obtain the approximate SEP expression

$$P_e \approx \left(\frac{\Theta}{2\pi} - \frac{1}{6} \right) M_\gamma(-c_{\text{MPSK}}) + \frac{1}{4} M_\gamma\left(-\frac{4c_{\text{MPSK}}}{3}\right) + \left(\frac{\Theta}{2\pi} - \frac{1}{4} \right) M_\gamma\left(-\frac{c_{\text{MPSK}}}{\sin^2\Theta}\right) . \quad (10)$$

Our numerical results will show that this approximation is accurate.

Note that both the exact SEP (5) and the approximate SEP (10) require the m.g.f. of the SINR γ . Although not shown, the same is true for M -QAM. This m.g.f. has been evaluated for Rayleigh fading scenarios [15], and in the following sections we evaluate it for more general practical cases including Rician fading.

IV. SINR RESULTS FOR RICIAN-RAYLEIGH FADING

This section considers the case where the desired user's signal is subject to Rician fading and the interferers are subject to Rayleigh fading. For example, this models a microcellular mobile system where the desired-user typically has LoS, but the interferers from neighboring cells do not. In this case, the desired-user channel vector \mathbf{c}_D is distributed according to

$$\mathbf{c}_D \sim \mathcal{CN}_{N_A,1}(\sqrt{a}\mathbf{m}, b\mathbf{I}_{N_A}) \quad (11)$$

where \mathbf{m} is the channel mean vector, satisfying $\|\mathbf{m}\|^2 = N_A$, and a and b are arbitrary coefficients used for power normalization purposes. The interference channels are distributed according to

$$\mathbf{C}_I \sim \mathcal{CN}_{N_A, N_I}(\mathbf{0}_{N_A \times N_I}, \mathbf{I}_{N_A} \otimes \mathbf{I}_{N_I}) . \quad (12)$$

A. SINR MGF for Rician-Rayleigh Fading

The following theorem applies for arbitrary numbers of interferers and antennas, and arbitrary signal, interferer, and noise powers.

Theorem 1: The SINR m.g.f. of an optimum combining system with Rician-faded users and Rayleigh-faded interferers is given by

$$M_\gamma(s) = K_1 \sum_{k=1}^{N_{\min}} (-1)^{k+1} \det(\mathbf{X}_k) \beta_k(s) \quad (13)$$

where

$$K_1 = \frac{(-1)^{N_A} (N_0/E_I)^\tau}{\Gamma_{N_{\min}}(N_{\min}) \Gamma_{N_{\min}}(N_{\max})} \quad (14)$$

where $N_{\min} = \min(N_A, N_I)$, $N_{\max} = \max(N_A, N_I)$, $\tau = N_A - N_{\min}$, and $\Gamma(\cdot)$ is the normalized complex multivariate gamma function¹ given by

$$\Gamma_{N_{\min}}(N_{\max}) = \prod_{i=1}^{N_{\min}} \Gamma(N_{\max} - i + 1) . \quad (15)$$

Also, $\beta_k(\cdot)$ is defined as

$$\beta_k(s) \triangleq \int_0^\infty x^{N_I - k} (N_0/E_I + x) e^{-x} h_1(s, x) dx - \sum_{t=1}^{\tau} \zeta_t(k+1) h_t(s, 0) \quad (16)$$

¹Note that this is related to the standard complex multivariate gamma function $\tilde{\Gamma}_N(M)$ (as defined in [21]) via $\Gamma_N(M) = \pi^{-N(N-1)/2} \tilde{\Gamma}_N(M)$.

$$\zeta_t(k) \triangleq (N_0/E_I) (N_I + t - k)! + (N_I + t - k + 1)! \quad (17)$$

$$h_t(s, x) \triangleq \frac{{}_1\mathcal{F}_1\left(t; N_A; \frac{aN_A s}{xE_I/E_D + N_0/E_D - bs}\right)}{(bsE_D/E_I - N_0/E_I - x)^t} \quad (18)$$

where ${}_1\mathcal{F}_1(\cdot)$ is the scalar confluent hypergeometric function, and \mathbf{X}_k corresponds to the $N_{\min} \times N_{\min}$ Hankel matrix \mathbf{X} with elements

$$\{\mathbf{X}\}_{i,j} = \zeta_{N_A}(i + j), \quad i, j = 1, \dots, N_{\min} \quad (19)$$

but with the first column and k^{th} row removed.

Proof: See Appendix I. □

We can see that the SINR m.g.f. depends on the Rician channel component only via the power scaling parameters a and b , and is independent of the mean vector \mathbf{m} . This reveals that the structure of \mathbf{m} has no impact on the statistics of the SINR, and therefore does not effect the system performance.

Note that (13)–(19) contains only standard functions, and therefore $M_\gamma(s)$ can be easily and efficiently evaluated numerically with software packages such as Maple and Mathematica (note that the hypergeometric function can be expressed as a finite sum involving only exponential and polynomial terms).

B. Special Case: Rayleigh-Rayleigh Fading

We now show how the general result of Theorem 1 simplifies for the special case of Rayleigh-Rayleigh fading. To the best of our knowledge, this result is new.

Corollary 1: For Rayleigh-Rayleigh fading, the SINR m.g.f. (13) reduces to

$$M_\gamma(s) = K_1 \sum_{k=1}^{N_{\min}} (-1)^k \det(\mathbf{X}_k) \beta_{N_I-k}(s) \quad (20)$$

where

$$K_1 = \frac{(-1)^{N_{\min}} (N_0/E_I)^\tau}{\Gamma_{N_{\min}}(N_{\min}) \Gamma_{N_{\min}}(N_{\max})} \quad (21)$$

$$\beta_t(s) = h_{t,\tau}(s) N_0/E_I + h_{t+1,\tau}(s) \quad (22)$$

$$h_{t,\tau}(s) = (t + \tau)! \kappa(s)^t e^{\kappa(s)} \Gamma(-(t + \tau), \kappa(s)) \quad (23)$$

$$\kappa(s) \triangleq N_0/E_I - sE_D/E_I, \quad (24)$$

where $\Gamma(\cdot, \cdot)$ is the incomplete gamma function, and \mathbf{X}_k is defined as in Theorem 1.

Proof: We first set $a = 0$ and $b = 1$ in Theorem 1; then evaluate the remaining integrals in closed-form using [15, eq. 16]; and finally perform simplifications using [24, eq. 6.5.19]. \square

Note that an alternative m.g.f. expression has also been derived for this Rayleigh-Rayleigh scenario in [15]. The result above, however, is simpler and easier to handle since it contains only simple scalar function of s , whereas the result from [15] involved more complicated determinant functions of s .

C. Moments of the SINR for Rician-Rayleigh Fading

The following theorem presents a closed-form expression for the moments of the SINR.

Theorem 2: The ℓ^{th} moment of the SINR of an OC system with Rician-faded users and Rayleigh-faded interferers is given by

$$\mu_\ell^{\text{Ric-Ray}} = \alpha_\ell^{\text{Ric}} \mu_\ell^{\text{Ray-Ray}} \quad (25)$$

where $\mu_\ell^{\text{Ray-Ray}}$ is the ℓ^{th} moment for an OC Rayleigh-Rayleigh system ($a = 0, b = 1$), given by

$$\mu_\ell^{\text{Ray-Ray}} = K_1 \sum_{k=1}^{N_{\min}} (-1)^k \det(\mathbf{X}_k) \xi_k \quad (26)$$

where

$$\begin{aligned} \xi_k &= \ell! (E_D/E_I)^\ell e^{N_0/E_I} \sum_{t=0}^{N_I-k} \binom{N_I-k}{t} (-N_0/E_I)^{N_I-k-t} \Gamma(t - \ell + 1, N_0/E_I) \\ &\quad + (E_D/N_0)^\ell \sum_{t=1}^{\tau} \zeta_t(k+1)(t)_\ell (-E_I/N_0)^t \end{aligned} \quad (27)$$

and K_1 , \mathbf{X}_k , and $\zeta_t(\cdot)$ are defined as in Theorem 1. Also, α_ℓ^{Ric} is a constant given by

$$\alpha_\ell^{\text{Ric}} = b^\ell \sum_{k=0}^{\ell} \binom{\ell}{k} \frac{(aN_A/b)^k}{(N_A)_k} \quad (28)$$

and $(N_A)_k = N_A(N_A + 1) \cdots (N_A + k - 1)$ is the Pochhammer symbol.

Proof: See Appendix II. \square

Given the intricacies of the derivation of $M_\gamma(s)$ in the proof of Theorem 1, it is remarkable to see that such a simple relationship exists between $\mu_\ell^{\text{Ric-Ray}}$ and $\mu_\ell^{\text{Ray-Ray}}$. To highlight the implications of this relationship, we now make the following remarks. Let us consider the common power normalization model with $a = K/(K + 1)$ and $b = 1/(K + 1)$, where K is the Rician K -factor.

Remark 1: The Rician component has *no effect on the average SINR*, since $\alpha_1^{\text{Ric}} = 1$.

Remark 2: The second moment of the SINR decreases monotonically with the Rician K -factor according to

$$\mu_2^{\text{Ric-Ray}} = \left(1 - \left(\frac{K}{K+1}\right)^2 \frac{1}{N_A + 1}\right) \mu_2^{\text{Ray-Ray}}. \quad (29)$$

Combined with Remark 1, this also shows that the variance of the SINR decreases monotonically with the Rician K -factor.

Remark 3: The ratio of SINR moments $\alpha_\ell^{\text{Ric}} = \mu_\ell^{\text{Ric-Ray}} / \mu_\ell^{\text{Ray-Ray}}$ depends *only* on the Rician K -factor and the number of antennas N_A , for all ℓ ; and is independent of the number of interferers N_I , the SNR E_D/N_0 , and the (normalized) signal-to-interference ratio (SIR) E_I/N_0 .

Remark 4: For fixed numbers of interferers N_I and antennas N_A , the SINR moments are bounded as a function of the Rician- K factor by

$$\left(\prod_{i=0}^{\ell-1} \frac{N_A}{N_A + i}\right) \mu_\ell^{\text{Ray-Ray}} \leq \mu_\ell^{\text{Ric-Ray}} \leq \mu_\ell^{\text{Ray-Ray}}, \quad (30)$$

for all ℓ , where the left-hand equality is approached as $K \rightarrow \infty$ (i.e. when the desired user's channel becomes nonfading), and the right-hand equality is met when $K \rightarrow 0$.

Remark 5: The SINR *distributions* for Rician-Rayleigh and Rayleigh-Rayleigh optimum combining systems are asymptotically equal as $N_A \rightarrow \infty$. This can be proved from (28) by showing

that all of the moments are asymptotically equal as follows:

$$\begin{aligned}
\lim_{N_A \rightarrow \infty} \mu_\ell^{\text{Ric-Ray}} / \mu_\ell^{\text{Ray-Ray}} &= \lim_{N_A \rightarrow \infty} \alpha_\ell^{\text{Ric}} \\
&= b^\ell \sum_{k=0}^{\ell} \binom{\ell}{k} (a/b)^k \lim_{N_A \rightarrow \infty} \left(\frac{N_A}{N_A} \right) \left(\frac{N_A}{N_A + 1} \right) \cdots \left(\frac{N_A}{N_A + k - 1} \right) \\
&= b^\ell \sum_{k=0}^{\ell} \binom{\ell}{k} (a/b)^k \\
&= (b + a)^\ell \\
&= 1
\end{aligned} \tag{31}$$

for all ℓ .

Remark 6: For large N_A , the Rayleigh-Rayleigh SINR moments satisfy

$$\mu_\ell^{\text{Ray-Ray}} = \left(\frac{E_D}{N_0} (N_A - N_I) \right)^\ell + \mathcal{O}(N_A^{\ell-1}), \tag{32}$$

which is obtained by taking N_A large in (26), and applying the following determinant identity for Hankel matrices: $\det(\{(N_{\max} + N_{\min} - i - j)!\}_{i,j=1}^{N_{\min}}) = \Gamma_{N_{\min}}(N_{\min}) \Gamma_{N_{\min}}(N_{\max})$. This shows that as the number of antennas grow, the Rayleigh-Rayleigh optimum combining system behaves like a nonfading AWGN system (with channel gain $N_A - N_I$). Combining this with Remark 4 above, we also make the same conclusion for Rician-Rayleigh systems.

V. SINR RESULTS FOR RAYLEIGH-RICIAN FADING

We now turn attention to the case where the desired-user's signal is subject to Rayleigh fading, and one or more of the interfering signals are subject to Rician fading (and the rest are Rayleigh fading). This situation applies to any multi-user or ad-hoc networking scenario when the desired user is Rayleigh. For example, this can be when they are far from the receiver. The model allows for some of the interferers to have LoS, but not necessarily all of the interferers, which is envisaged to be a fairly common scenario in practice.

In this case, the user channel vector \mathbf{c}_D is distributed according to

$$\mathbf{c}_D \sim \mathcal{CN}_{N_A,1}(\mathbf{0}_{N_A \times 1}, \mathbf{I}_{N_A}). \tag{33}$$

The interference channels are distributed according to

$$\mathbf{C}_I \sim \mathcal{CN}_{N_A, N_I}(\sqrt{a}\mathbf{M}, b\mathbf{I}_{N_A} \otimes \mathbf{I}_{N_I}) \tag{34}$$

where a and b are arbitrary coefficients, and \mathbf{M} is an arbitrary deterministic matrix (possibly with zero-valued columns, allowing for any number of the interferers to be Rician), normalized such that $\text{tr}(\mathbf{M}\mathbf{M}^\dagger) = N_A N_I$. It is important to note that we place no restrictions on the structure of \mathbf{M} , other than a power normalization.

A. SINR MGF for Rayleigh-Rician Fading

Theorem 3: The SINR m.g.f. of an optimum combining system with Rayleigh-faded users and Rician-faded interferers is given by

$$M_\gamma(s) = K_2 A(s) \sum_{k=1}^{N_{\min}} (-1)^{N_{\min}+k} \det(\mathbf{Y}_k) \varrho_k(s) \quad (35)$$

where K_2 and $A(\cdot)$ are given by

$$K_2 = \frac{e^{-\text{tr}(\Theta)}}{\Gamma_{N_{\min}-L}(N_{\min}-L) \Gamma_{N_{\min}-L}(N_{\max}-L) V_L(\Theta) \prod_{k=1}^L \theta_k^{N_{\min}-L}} \quad (36)$$

and

$$A(s) \triangleq (1 - sE_D/N_0)^{-\tau}, \quad (37)$$

respectively, $\delta = N_{\max} - N_{\min}$, and $\theta_1 > \theta_2 > \dots > \theta_L$ are the non-zero eigenvalues of

$$\Theta = \frac{a}{b} \mathbf{M}\mathbf{M}^\dagger. \quad (38)$$

The function $V_L(\cdot)$ is a Vandermonde determinant in the L non-zero eigenvalues of the matrix argument, given by²

$$V_L(\Theta) = \prod_{i<j}^L (\theta_i - \theta_j) = \det\left(\{\theta_i^{L-j}\}_{i,j=1}^L\right), \quad (39)$$

and $\varrho_k(\cdot)$ is defined as

$$\varrho_k(s) \triangleq \begin{cases} \int_0^\infty \frac{(x/\theta_k)^{\delta/2} e^{-x} I_\delta(2\sqrt{\theta_k x})}{1 - \frac{sE_D}{bE_I x + N_0}} dx, & k = 1, \dots, L \\ h_{N_{\max}-k+1,0}(s) + \left(\frac{N_0}{bE_I}\right) h_{N_{\max}-k,0}(s), & k = L+1, \dots, N_{\min} \end{cases} \quad (40)$$

²For notational convenience, we will sometimes give a set in place of a matrix in the argument of $V_L(\cdot)$, as a shorthand. Specifically, for the set \mathcal{A} , we use $V_L(\mathcal{A})$ as shorthand for $V_L(\text{diag}(\mathcal{A}))$.

where $I_\delta(\cdot)$ is the modified Bessel function of the first kind, and $h_{t,0}(\cdot)$ is defined as in (23).

Also, \mathbf{Y}_k corresponds to the $N_{\min} \times N_{\min}$ matrix \mathbf{Y} with elements

$$\{\mathbf{Y}\}_{i,j} = \begin{cases} g_{N_{\max}-j+1}(\theta_i) + \left(\frac{N_0}{bE_I}\right) g_{N_{\max}-j}(\theta_i) & i = 1, \dots, L, \quad j = 1, \dots, N_{\min} \\ \zeta(i+j-1) + \left(\frac{N_0}{bE_I}\right) \zeta(i+j), & i = L+1, \dots, N_{\min}, \quad j = 1, \dots, N_{\min} \end{cases} \quad (41)$$

where

$$g_t(\theta_i) \triangleq t! e^{\theta_i} \sum_{r=0}^{t-\delta} \binom{t-\delta}{r} \frac{\theta_i^r}{(\delta+r)!} \quad (42)$$

$$\zeta(t) \triangleq (N_A + N_I - t)! \quad , \quad (43)$$

but with the first column and k^{th} row removed.

Proof: See Appendix III. □

It is important to emphasize that, as with the previous theorems, the m.g.f. in (35) involves only simple scalar functions of s , and that it contains only standard functions and can be easily and efficiently evaluated numerically.

Note also that the SINR moments for this Rayleigh-Rician scenario can be obtained via differentiation of (35). In contrast to the Rician-Rayleigh moments given in the previous section, however, these moments only admit an integral or infinite series solution - thus we omit the analysis here. Finally, we mention that for the case $a = 0$ and $b = 1$, the m.g.f. in (35) can be easily shown to reduce to the Rayleigh-Rayleigh m.g.f. presented in Section IV-B.

VI. NUMERICAL RESULTS

We now validate the preceding theoretical analysis and examine the effect of the various system/channel parameters. Throughout this section we define $\text{SIR} = E_D/(N_I E_I)$, and $\text{SNR} = E_D/N_0$. We also assume the common Rician fading power normalization strategy, with $a = K/(K+1)$ and $b = 1/(K+1)$, where K corresponds to the Rician K -factor.

A. Rician-Rayleigh Fading

Recall that in this case we have shown that the specific choice of \mathbf{m} has no effect on the system performance, and as such, for all simulation results presented in this subsection, the mean vector \mathbf{m} was randomly-generated.

Fig. 1 shows analytical and Monte-Carlo simulated SEP curves for a Rician-Rayleigh OC system, comparing BPSK and 8-PSK modulation, and different N_I . The “Analytical (Exact)” curves were generated by combining (13) and (5), and the “Analytical (Approx)” curves were generated by combining (13) and (10). We see that in all cases the “Analytical (Exact)” SEP curves match precisely with the simulated curves, and that the “Analytical (Approx)” curves are accurate. For both modulation schemes, we also observe that an error floor exists when the number of interferers exceeds the number of degrees of freedom of the array (i.e. $N_A - 1$), which aligns with well-established results for Rayleigh-Rayleigh systems (see, e.g., [7]).

Fig. 2 shows the analytical and Monte-Carlo simulated SEP curves for a system with $SIR = 0$ dB and $SIR = 10$ dB, and for different Rician K -factors. Again, we see that in all cases the “Analytical (Exact)” curves match precisely with the simulated curves, and the “Analytical (Approx)” curves are accurate. For both SIRs, we also observe that the SEP improves with increasing K . The relative improvement is most significant for the higher SIR.

Fig. 3 further investigates the impact of the Rician K -factor on the SEP performance, comparing systems with $N_A = 2$ and $N_A = 3$, for a range of SIRs. The curves were generated based on the exact analytical SEP results, obtained by combining (13) and (5). Note that each curve essentially shows how the SEP performance varies as the desired-user channel undergoes a transition from Rayleigh fading ($K = 0$) to a deterministic nonfading channel ($K \rightarrow \infty$). We see that, in all cases, the SEP decreases monotonically with K , and the rate of decrease is most significant for low K values (e.g. < 5). We also see that K has the most impact for high SIRs (as suggested from Fig. 2) and that the relative effect of K appears to be independent of the number of antennas.

Fig. 4 shows analytical and Monte-Carlo simulated curves for the second moment of the SINR as a function of K ; comparing different N_I . The “Analytical” curves were generated using (25). In all cases we see a precise agreement between the analysis and simulations. Also, as predicted from Section IV-C (see Remarks 2 and 4), we see that for all values of N_I this moment decreases monotonically with K ; eventually converging to a deterministic constant.

Fig. 5 shows the ratio of the SINR moments of a Rician-Rayleigh and Rayleigh-Rayleigh system α_ℓ^{Ric} (defined in (28)) as a function of K , for the first, second, and third moments, and for $N_A = 2, 3$, and 4. Recall that this ratio is independent of the SNR, SIR, and N_I . As suggested in Section IV-C (see Remark 1), we see that the Rician- K factor has no effect on the average

SINR. We see that the second and third moments, however, decrease monotonically with K - this is most significant for the third moment. Moreover, for the second and third moments, we see that the effect of K becomes less significant (and α_ℓ^{Ric} becomes closer to 1) as N_A increases. This behavior is also consistent with the analytic conclusions given in Section IV-C (Remark 5).

B. Rayleigh-Rician Fading

In the Rayleigh-Rician case the mean matrix \mathbf{M} is constructed by using the model in [25, eq. 6] for each Rician interferer. Unless otherwise indicated, throughout this section we assume that two of the interfering users are Rician. Note that this is simply by way of example. In this case, the mean is constructed according to $\mathbf{M} = [\mathbf{a}(\bar{\theta}_{R_1}), \mathbf{a}(\bar{\theta}_{R_2}), \mathbf{0}_{N_A \times (N_1 - 2)}]$, where $\mathbf{a}(\bar{\theta}_{R_i}) = [1, e^{j2\pi\Delta \cos(\bar{\theta}_{R_i})}, \dots, e^{j2\pi\Delta(N_A - 1) \cos(\bar{\theta}_{R_i})}]$ is the array response vector for the i th Rician interferer. This vector models the phase shift as the LoS component traverses the receive array, and depends on the angle of arrival (AoA) $\bar{\theta}_{R_i}$ and the relative antenna spacing Δ (in terms of the wavelength). We choose $\Delta = 1/2$, $\bar{\theta}_{R_1} = \pi/4$, and $\bar{\theta}_{R_2} = \pi/5$. Again, this is simply by way of example; and different AOAs and antenna spacings could just as easily have been considered.

Fig. 6 shows analytical and Monte-Carlo simulated SEP curves for a Rayleigh-Rician OC system, comparing different N_1 . Note that, for the case of $N_1 = 1$, only the Rician interferer with AoA equal to $\pi/4$ was considered. The ‘‘Analytical (Exact)’’ curves were generated by combining (35) and (5), and the ‘‘Analytical (Approx)’’ curves were generated by combining (35) and (10). We see that in all cases the ‘‘Analytical (Exact)’’ SEP curves match precisely with the simulated curves, and that the ‘‘Analytical (Approx)’’ curves are accurate. As expected, when $N_1 < N_A$ the curve does not exhibit an error floor, since there are enough degrees of freedom to cancel all the interferers. Fig. 7 gives results for different SIR. Clearly the approximation holds for a wide range of SIRs.

Fig. 8 shows the SEP as a function of the ratio between the two nonzero eigenvalues θ_1 and θ_2 of Θ , defined in (38), for different values of the Rician K -factor. When θ_2/θ_1 is small, Θ is close to rank-1, which means there is a single strong direction of interference. As the K -factor increases, this interference direction dominates. Clearly, the figure shows that in this case the performance improves with K -factor, indicating that it is easier to cancel a single dominant interferer than it is to cancel many Rayleigh components (of course recall that we are operating under a power normalization such that the total average received power is the same in all cases).

The case of θ_2/θ_1 close to one, corresponds to having two dominant Rician paths which are orthogonal. Clearly this is the hardest interference case for the combiner to deal with. The figure shows that in this case the performance degrades with K -factor, indicating that it is harder to cancel these Rician paths than it is to cancel many Rayleigh components.

VII. CONCLUSIONS

This paper considered the analysis of Rician-Rayleigh and Rayleigh-Rician OC systems in the presence of interference and noise. Exact expressions were derived for the m.g.f. of the SINR, which were used to examine the SEP. For the Rician-Rayleigh case, exact insightful closed-form expressions were also derived for the moments of the SINR. Our results have demonstrated that Rician fading has a beneficial impact on the performance of OC systems.

APPENDIX I

PROOF OF THEOREM 1

Proof: We evaluate the SINR m.g.f. in two stages. We first derive the m.g.f. when conditioned on the interference channel gains \mathbf{C}_I (equivalently \mathbf{R}); then average over the interference channel statistics.

Note that a similar approach was used in [6, 11] for the SINR m.g.f. calculation of OC systems in Rayleigh-Rayleigh channels. The Rician-Rayleigh analysis here however, is significantly more complicated for two main reasons. First, with c_D distributed according to (11), the conditional m.g.f. corresponds to the m.g.f. of a noncentral quadratic form in complex Gaussian random vectors, whereas for the Rayleigh-Rayleigh case more convenient central quadratic form expressions can be used. Second, as we will see, to calculate the unconditional Rician-Rayleigh m.g.f., we will need to integrate over both the distribution of the eigenvalues and eigenvectors of \mathbf{C}_I . For the Rayleigh-Rayleigh case, this step is simplified by exploiting the unitary-invariance property of the desired-user channel vector c_D .

We start our analysis by employing the general noncentral quadratic form m.g.f. result from [26, App. B], along with (3), to write

$$M_\gamma(s) = \mathbb{E}_{\tilde{\mathbf{R}}} [M_{\gamma|\tilde{\mathbf{R}}}(s)] = \mathbb{E}_{\tilde{\mathbf{R}}} \left[\frac{\exp \left(-\frac{a}{b} \mathbf{m}^\dagger \left(\left(1 - \frac{N_0}{E_I \bar{s}} \right) \mathbf{I}_{N_A} - \frac{1}{\bar{s}} \tilde{\mathbf{R}} \right)^{-1} \mathbf{m} \right)}{\det \left(\mathbf{I}_{N_A} - \bar{s} \left(\frac{N_0}{E_I} \mathbf{I}_{N_A} + \tilde{\mathbf{R}} \right)^{-1} \right)} \right] \quad (44)$$

where

$$\bar{s} = bsE_D/E_I \quad (45)$$

and $\tilde{\mathbf{R}} \triangleq \mathbf{C}_1\mathbf{C}_1^\dagger$. The major challenge here is to perform the averaging over $\tilde{\mathbf{R}}$.

Let us first define

$$\mathbf{Y} \triangleq \left(\left(1 - \frac{N_0}{E_I \bar{s}} \right) \mathbf{I}_{N_A} - \frac{1}{\bar{s}} \tilde{\mathbf{R}} \right)^{-1}. \quad (46)$$

Since $\tilde{\mathbf{R}}$ and \mathbf{Y} are both Hermitian, they admit the following eigenvalue decompositions:

$$\begin{aligned} \tilde{\mathbf{R}} &= \mathbf{U}_{\tilde{\mathbf{R}}} \mathbf{\Lambda}_{\tilde{\mathbf{R}}} \mathbf{U}_{\tilde{\mathbf{R}}}^\dagger, & \mathbf{\Lambda}_{\tilde{\mathbf{R}}} &= \text{diag}(\lambda_1, \dots, \lambda_{N_A}), & \mathbf{U}_{\tilde{\mathbf{R}}} &\in \mathcal{U}(N_A) \\ \mathbf{Y} &= \mathbf{U}_Y \mathbf{\Lambda}_Y \mathbf{U}_Y^\dagger, & \mathbf{\Lambda}_Y &= \text{diag}(\tilde{\lambda}_1, \dots, \tilde{\lambda}_{N_A}), & \mathbf{U}_Y &\in \mathcal{U}(N_A) \end{aligned} \quad (47)$$

where $0 = \lambda_{N_A} = \dots = \lambda_{N_{\min}+1} < \lambda_{N_{\min}} \leq \dots \leq \lambda_1 < \infty$ are the ordered eigenvalues of $\tilde{\mathbf{R}}$, and $\mathcal{U}(N_A)$ is the unitary manifold consisting of $N_A \times N_A$ unitary matrices with real diagonal elements. It can be easily verified from (46) that

$$\mathbf{U}_Y = \mathbf{U}_{\tilde{\mathbf{R}}} \quad (48)$$

and

$$\mathbf{\Lambda}_Y = \text{diag}(\{\tilde{\lambda}_i\}_{i=1, \dots, N_A}) = \text{diag} \left(\left\{ \frac{\bar{s}}{\bar{s} - N_0/E_I - \lambda_i} \right\}_{i=1, \dots, N_A} \right). \quad (49)$$

Using (46)-(48), we can write the exponential in the numerator of (44) as follows

$$\exp \left(-\frac{a}{b} \mathbf{m}^\dagger \mathbf{Y} \mathbf{m} \right) = \exp \left(-\text{tr} \left(\mathbf{B} \mathbf{U}_{\tilde{\mathbf{R}}} \mathbf{\Lambda}_Y \mathbf{U}_{\tilde{\mathbf{R}}}^\dagger \right) \right) \quad (50)$$

where $\mathbf{B} = \frac{a}{b} \mathbf{m} \mathbf{m}^\dagger$. The denominator determinant in (44) can also be written as

$$\det \left(\mathbf{I}_{N_A} - \bar{s} \left(\frac{N_0}{E_I} \mathbf{I}_{N_A} + \tilde{\mathbf{R}} \right)^{-1} \right) = \left(1 - \frac{\bar{s}}{N_0/E_I} \right)^\tau \prod_{i=1}^{N_{\min}} \left(1 - \frac{\bar{s}}{N_0/E_I + \lambda_i} \right) \quad (51)$$

and thus the m.g.f. in (44) can be expressed as

$$M_\gamma(s) = \left(\frac{N_0/E_I}{N_0/E_I - \bar{s}} \right)^\tau \mathbb{E}_{\mathbf{\Lambda}_{\tilde{\mathbf{R}}}} \left[\prod_{i=1}^{N_{\min}} \left(\frac{N_0/E_I + \lambda_i}{N_0/E_I + \lambda_i - \bar{s}} \right) \mathcal{I}(\mathbf{\Lambda}_{\tilde{\mathbf{R}}}) \right] \quad (52)$$

where

$$\mathcal{I}(\mathbf{\Lambda}_{\tilde{\mathbf{R}}}) = \int_{\mathcal{U}(N_A)} \exp \left(-\text{tr} \left(\mathbf{B} \mathbf{U}_{\tilde{\mathbf{R}}} \mathbf{\Lambda}_Y \mathbf{U}_{\tilde{\mathbf{R}}}^\dagger \right) \right) [d\mathbf{U}_{\tilde{\mathbf{R}}}] \quad (53)$$

where $[d\mathbf{U}_{\tilde{R}}]$ is the normalized Haar invariant probability measure on $\mathcal{U}(N_A)$. To evaluate (53), we force both \mathbf{B} and $\mathbf{\Lambda}_{\tilde{R}}$ to be full-rank by perturbing all of the zero-valued eigenvalues. These eigenvalues will subsequently be driven back to zero. We can then use the identity [21, eq. (89)] and the splitting property of hypergeometric functions [21, eq. (92)] to perform the integration in (53) as follows

$$\mathcal{I}(\mathbf{\Lambda}_{\tilde{R}}) = \int_{\mathcal{U}(N_A)} {}_0\mathcal{F}_0 \left(-\mathbf{B}\mathbf{U}_{\tilde{R}}\mathbf{\Lambda}_Y\mathbf{U}_{\tilde{R}}^\dagger \right) [d\mathbf{U}_{\tilde{R}}] = {}_0\mathcal{F}_0(\mathbf{B}, -\mathbf{\Lambda}_Y) . \quad (54)$$

Now, noting that the N_A eigenvalues of \mathbf{B} are given by $\{a\|\mathbf{m}\|^2/b, 0, \dots, 0\}$, we can invoke [27, Corr. 1] to write ${}_0\mathcal{F}_0(\cdot)$ in a determinant form which accounts for the zero-valued eigenvalues of \mathbf{B} . Then, recalling that $\|\mathbf{m}\|^2 = N_A$, we perform some simplifications using (49) to obtain

$$\mathcal{I}(\mathbf{\Lambda}_{\tilde{R}}) = \frac{\Gamma(N_A)(-\bar{s})^{(N_A-1)(N_A-2)/2} \det(\mathbf{G})}{(aN_A/b)^{N_A-1} V_{N_A}(-\mathbf{\Lambda}_Y)} \quad (55)$$

where $V_{N_A}(\cdot)$ is a Vandermonde determinant, defined in (39), and \mathbf{G} is an $N_A \times N_A$ matrix with $(i, j)^{\text{th}}$ element given by

$$\{\mathbf{G}\}_{i,j} = \begin{cases} \exp\left(-\frac{aN_A\bar{s}/b}{w(\bar{s}, \lambda_i)}\right), & i = 1, \dots, N_A, \quad j = 1 \\ w(\bar{s}, \lambda_i)^{j-N_A}, & i = 1, \dots, N_A, \quad j = 2, \dots, N_A \end{cases} \quad (56)$$

where

$$w(\bar{s}, \lambda_i) = \bar{s} - \lambda_i - N_0/E_1 . \quad (57)$$

We now manipulate the Vandermonde determinant in the denominator of (55) using the identity [28, eq. (56)], and noting that $V_n(\{c + x_i\}) = V_n(\{x_i\})$ for any constant c , which yields

$$\mathcal{I}(\mathbf{\Lambda}_{\tilde{R}}) = \frac{\Gamma(N_A) \prod_{i=1}^{N_A} w(\bar{s}, \lambda_i)^{N_A-1} \det(\mathbf{G})}{(-aN_A\bar{s}/b)^{N_A-1} V_{N_A}(\mathbf{\Lambda}_{\tilde{R}})} . \quad (58)$$

In order to avoid numerical instability for small values of a (i.e. near-Rayleigh scenarios) and small values of s , we find it useful to absorb the leading factors into the determinant as follows

$$\mathcal{I}(\mathbf{\Lambda}_{\tilde{R}}) = \frac{\det(\mathbf{F})}{V_{N_A}(\mathbf{\Lambda}_{\tilde{R}})} \quad (59)$$

where \mathbf{F} has $(i, j)^{\text{th}}$ element

$$\{\mathbf{F}\}_{i,j} = \begin{cases} \Gamma(N_A) \left(-\frac{w(\bar{s}, \lambda_i)}{aN_A\bar{s}/b}\right)^{N_A-1} \exp\left(-\frac{aN_A\bar{s}/b}{w(\bar{s}, \lambda_i)}\right), & i = 1, \dots, N_A, \quad j = 1 \\ w(\bar{s}, \lambda_i)^{j-1}, & i = 1, \dots, N_A, \quad j = 2, \dots, N_A \end{cases} \quad (60)$$

We can simplify the elements in the first column of \mathbf{F} by expanding the exponential to give

$$\{\mathbf{F}\}_{i,j} = \Gamma(N_A) \sum_{\ell=0}^{\infty} \frac{\left(-\frac{aN_A\bar{s}/b}{w(\bar{s},\lambda_i)}\right)^{\ell-N_A+1}}{\ell!}, \quad i = 1, \dots, N_A, \quad j = 1 \quad (61)$$

and noting that the terms in the sum corresponding to $\ell = 0, \dots, N_A - 2$ can be neglected as they are constant multiples of elements in columns $j = 2, \dots, N_A$. Thus we obtain

$$\{\mathbf{F}\}_{i,j} = \Gamma(N_A) \sum_{\ell=N_A-1}^{\infty} \frac{\left(-\frac{aN_A\bar{s}/b}{w(\bar{s},\lambda_i)}\right)^{\ell-N_A+1}}{\ell!} \quad (62)$$

$$= {}_1\mathcal{F}_1\left(1; N_A; -\frac{aN_A\bar{s}/b}{w(\bar{s},\lambda_i)}\right), \quad i = 1, \dots, N_A, \quad j = 1 \quad (63)$$

We can also simplify the elements in columns $j = 2, \dots, N_A$. To this end, we first remove $w(\bar{s}, \lambda_i)$ from each row such that, from (57), the elements in column $j \in \{2, \dots, N_A\}$ are polynomials (in the λ_i s) of degree $j - 2$. We then proceed from columns $j = 3$ to $j = N_A$ (in order), at each stage subtracting scalar multiples of columns $2, \dots, j - 1$ to remove all lower order polynomial terms (this has no effect on the value of the determinant). Finally we perform some column swaps to obtain

$$\mathcal{I}(\mathbf{\Lambda}_{\tilde{R}}) = \prod_{i=1}^{N_A} w(\bar{s}, \lambda_i) \frac{\det(\mathbf{H})}{V_{N_A}(\mathbf{\Lambda}_{\tilde{R}})} \quad (64)$$

where \mathbf{H} has $(i, j)^{\text{th}}$ element

$$\{\mathbf{H}\}_{i,j} = \begin{cases} \frac{{}_1\mathcal{F}_1\left(1; N_A; -\frac{aN_A\bar{s}/b}{w(\bar{s},\lambda_i)}\right)}{w(\bar{s},\lambda_i)}, & i = 1, \dots, N_A, \quad j = 1 \\ \lambda_i^{N_A-j}, & i = 1, \dots, N_A, \quad j = 2, \dots, N_A \end{cases} \quad (65)$$

Recall that we must still take the limits $\lambda_i \rightarrow 0$, for $i = N_{\min} + 1, \dots, N_A$. To this end, we can apply the general limiting result in [27, Corr. 1] to (64) and, after lengthy algebraic manipulations, evaluate these limits to yield

$$\mathcal{I}(\mathbf{\Lambda}_{\tilde{R}}) = w(\bar{s}, 0)^\tau \left(\prod_{i=1}^{N_{\min}} \frac{w(\bar{s}, \lambda_i)}{\lambda_i^\tau} \right) \frac{\det(\mathbf{J})}{V_{N_{\min}}(\mathbf{\Lambda}_{\tilde{R}})} \quad (66)$$

where \mathbf{J} is an $N_{\min} \times N_{\min}$ matrix with elements

$$\{\mathbf{J}\}_{i,j} = \begin{cases} h_1(s, \lambda_i) - \sum_{t=1}^{\tau} h_t(s, 0) \lambda_i^{t-1}, & i = 1, \dots, N_{\min}, \quad j = 1 \\ \lambda_i^{N_A-j}, & i = 1, \dots, N_{\min}, \quad j = 2, \dots, N_{\min} \end{cases} \quad (67)$$

where $h_t(\cdot, \cdot)$ is defined in (18). Now substituting (66) into (52), the m.g.f. becomes

$$M_\gamma(s) = (-1)^{N_A} (N_0/E_1)^\tau \mathbb{E}_{\Lambda_{\tilde{R}}} \left[\left(\prod_{i=1}^{N_{\min}} \frac{(N_0/E_1 + \lambda_i)}{\lambda_i^\tau} \right) \frac{\det(\mathbf{J})}{V_{N_{\min}}(\Lambda_{\tilde{R}})} \right]. \quad (68)$$

We see that the remaining expectation is over the N_{\min} *non-zero* ordered eigenvalues of $\tilde{\mathbf{R}}$. These eigenvalues have the same distribution as the ordered eigenvalues of a complex Wishart matrix of dimension $N_{\min} \times N_{\min}$, and with N_{\max} degrees of freedom, and thus have the following p.d.f.:

$$f_{\text{ord}}(\lambda_1, \dots, \lambda_{N_{\min}}) = \frac{\prod_{i=1}^{N_{\min}} (e^{-\lambda_i} \lambda_i^{N_{\max} - N_{\min}}) V_{N_{\min}}(\Lambda_{\tilde{R}})^2}{\Gamma_{N_{\min}}(N_{\min}) \Gamma_{N_{\min}}(N_{\max})}. \quad (69)$$

Using (69) in (68) and noting that $V_{N_{\min}}(\Lambda_{\tilde{R}}) = \det(\{\lambda_i^{N_{\min}-j}\}_{i,j=1}^{N_{\min}})$, we obtain

$$M_\gamma(s) = K_1 \int \cdots \int_{\mathcal{D}} \det(\{\lambda_i^{N_{\min}-j}\}_{i,j=1}^{N_{\min}}) \det(\mathbf{J}) \prod_{i=1}^{N_{\min}} g(\lambda_i) d\lambda \quad (70)$$

where $d\lambda = d\lambda_1 d\lambda_2 \dots d\lambda_{N_{\min}}$, the multiple integral is over the domain $\mathcal{D} = \{\infty \geq \lambda_1 \geq \dots \geq \lambda_{N_{\min}} \geq 0\}$, K_1 is defined in (14), and $g(\lambda_i) = (N_0/E_1 + \lambda_i) \lambda_i^{N_{\max} - N_A} e^{-\lambda_i}$.

The theorem now follows by applying the general integration identity [29, Corr. 2] to (70), performing some subsequent simplifications to the resulting determinant using [30, eq. 3.381.4], and then finally applying Laplace's expansion along the first column. □

APPENDIX II

PROOF OF THEOREM 2

Proof: The ℓ^{th} moment of the SINR can be evaluated from the m.g.f. in (13) via

$$\mu_\ell^{\text{Ric-Ray}} = \frac{d^\ell}{ds^\ell} M_\gamma(s) \Big|_{s=0} = K_1 \sum_{k=1}^{N_{\min}} (-1)^{k+1} \det(\mathbf{X}_k) \frac{d^\ell}{ds^\ell} \beta_k(s) \Big|_{s=0} \quad (71)$$

where

$$\frac{d^\ell}{ds^\ell} \beta_k(s) \Big|_{s=0} = \int_0^\infty x^{N_1-k} (N_0/E_1 + x) e^{-x} \frac{d^\ell}{ds^\ell} h_1(s, x) \Big|_{s=0} dx - \sum_{t=1}^{\tau} \zeta_t(k+1) \frac{d^\ell}{ds^\ell} h_t(s, 0) \Big|_{s=0}. \quad (72)$$

Note that, in deriving (72) from (71) and (16), we have exchanged the ℓ -derivative and integral in the right-hand term. This exchange can be easily justified via the Dominated Convergence

Theorem. After some manipulations, we evaluate the derivatives in (72) to yield

$$\frac{d^\ell}{ds^\ell} \beta_k(s) \Big|_{s=0} = -\alpha_\ell^{\text{Ric}} \ell! \left(\frac{E_D}{E_1} \right)^\ell \int_0^\infty \frac{x^{N_1-k} e^{-x}}{(x + N_0/E_1)^\ell} dx - \sum_{t=1}^{\tau} \alpha_\ell^{\text{Ric}} \zeta_t(k+1)(t)_\ell \left(-\frac{E_1}{N_0} \right)^t \left(\frac{E_D}{N_0} \right)^\ell. \quad (73)$$

We now evaluate the remaining integral in closed-form by applying a simple transformation, along with the binomial theorem, to obtain

$$\int_0^\infty \frac{x^{N_1-k} e^{-x}}{(x + N_0/E_1)^\ell} dx = e^{N_0/E_1} \sum_{t=0}^{N_1-k} \binom{N_1-k}{t} \left(-\frac{N_0}{E_1} \right)^{N_1-k-t} \Gamma(t - \ell + 1, N_0/E_1). \quad (74)$$

The proof is completed by combining (74), (73) and (71). \square

APPENDIX III

PROOF OF THEOREM 3

Proof: We first evaluate the m.g.f. when conditioned on the interference channel gains \mathbf{C}_I (equivalently \mathbf{R}); then average over the interference channel statistics.

Note that the main challenge of this derivation, in comparison to the Rayleigh-Rayleigh m.g.f. derivations considered previously in [6, 11], is that it involves eigenvalue distributions of complex non-central Wishart matrices, rather than the more convenient central Wishart distributions used in [6, 11].

We start by noting that since c_D exhibits Rayleigh fading (and is thus invariant under unitary transformation), the conditional m.g.f. can be directly inferred from [7] as

$$M_{\gamma|\mathbf{R}}(s) = A(s) \prod_{i=1}^{N_{\min}} \left(1 - \frac{sE_D}{E_1\lambda_i + N_0} \right)^{-1} \quad (75)$$

where $\lambda_1 \geq \dots \geq \lambda_{N_{\min}}$ are the nonzero ordered eigenvalues of $\mathbf{C}_I \mathbf{C}_I^\dagger$.

The main challenge is to remove the conditioning in (75). To this end, let us first define $\mathbf{x} = (x_1, \dots, x_{N_{\min}})$, with

$$x_i = \lambda_i/b. \quad (76)$$

Note that, with \mathbf{C}_I distributed according to (34), the x_i 's have the same distribution as the ordered eigenvalues of a complex noncentral Wishart matrix $\mathbf{X} \sim \mathcal{W}_{N_{\min}}(N_{\max}, \mathbf{I}_{N_{\min}}, \Theta)$, with

non-centrality matrix Θ defined in (38). For the general case considered in this paper where \mathbf{M} (and thus Θ) is allowed arbitrary-rank, this eigenvalue distribution is given by [31]

$$f_{\mathbf{x}}(x_1, \dots, x_{N_{\min}}) = K_2 \left(\prod_{k=1}^{N_{\min}} x_k^\delta e^{-x_k} \right) \det \left(\{x_i^{N_{\min}-j}\}_{i,j=1}^{N_{\min}} \right) \det(\mathbf{T}) \quad (77)$$

where \mathbf{T} is an $N_{\min} \times N_{\min}$ matrix with $(i, j)^{\text{th}}$ element

$$\{\mathbf{T}\}_{i,j} = \begin{cases} {}_0\mathcal{F}_1(\delta + 1, \theta_j x_i) / \delta!, & i = 1, \dots, N_{\min}, \quad j = 1, \dots, L \\ x_i^{N_{\min}-j}, & i = 1, \dots, N_{\min}, \quad j = L + 1, \dots, N_{\min} \end{cases} \quad (78)$$

Thus, combining (76) and (75), and using (77), the unconditional m.g.f. can be written as

$$M_\gamma(s) = K_2 A(s) \int \cdots \int_D \left(\prod_{k=1}^{N_{\min}} g(x_k) \right) \det \left(\{x_i^{N_{\min}-j}\}_{i,j=1}^{N_{\min}} \right) \det(\mathbf{T}) d\mathbf{x} \quad (79)$$

where the multiple integral is over the domain $\mathcal{D} = \{\infty > x_1 \geq \cdots \geq x_{N_{\min}} > 0\}$, with $d\mathbf{x} = dx_1 \cdots dx_{N_{\min}}$, and $g(\cdot)$ is given by

$$g(x) = \frac{x^\delta e^{-x} (x + N_0 / (bE_1))}{x + \kappa(s)} \quad (80)$$

where $\kappa(s)$ is defined in (24).

At this point, we could directly simplify the multiple integral in (79) by invoking the general integration identity [29, Corr. 2]. Since $g(\cdot)$ depends on s , however, the result would involve a determinant of a matrix with all elements as functions of s , and would also require the numerical evaluation of $N_{\min} \times L$ integrals. We now show that the result can be greatly simplified to an expression involving only a scalar function of s (as in Theorem 1), and which only requires the numerical evaluation of L integrals. The key step is to express the Vandermonde determinant in (79) as follows

$$\det \left(\{x_i^{N_{\min}-j}\}_{i,j=1}^{N_{\min}} \right) = (-1)^{N_{\min}-1} \prod_{k=1}^{N_{\min}} (\kappa(s) + x_k) \det(\mathbf{A}) \quad (81)$$

where \mathbf{A} is an $N_{\min} \times N_{\min}$ matrix with $(i, j)^{\text{th}}$ element

$$\{\mathbf{A}\}_{i,j} = \begin{cases} (\kappa(s) + x_i)^{-1}, & i = 1, \dots, N_{\min}, \quad j = 1 \\ x_i^{N_{\min}-j}, & i = 1, \dots, N_{\min}, \quad j = 2, \dots, N_{\min} \end{cases} \quad (82)$$

Note that this result can be proven, starting from the right-hand side, by multiplying the i^{th} row of \mathbf{A} by $(\kappa(s) + x_i)$, and then performing some simple column operations to remove low order polynomial terms. Now we substitute (81) into (79), and see that the denominator factor in $g(\cdot)$

cancels. We then apply the integration identity [29, Corr. 2]; simplify the resulting determinant using [24, eq. 9.6.47]; and perform a Laplace expansion along the first column. This yields

$$M_\gamma(s) = K_2 A(s) \sum_{k=1}^{N_{\min}} (-1)^{N_{\min}+k} \det(\mathbf{Y}_k) \varrho_k(s) \quad (83)$$

where $\varrho_k(s)$ and \mathbf{Y}_k are defined in the theorem, but with

$$h_t(s) = \int_0^\infty \frac{x^t e^{-x}}{\kappa(s) + x} dx \quad (84)$$

$$g_t(\theta_i) = \theta_i^{-\delta/2} \int_0^\infty x^{t-\delta/2} e^{-x} I_\delta(2\sqrt{\theta_i x}) dx \quad (85)$$

$$\zeta(t) = \int_0^\infty x^{N_A+N_1-t} e^{-x} dx \quad (86)$$

The theorem now follows by evaluating the integrals in (84), (85) and (86) in closed-form using the identities [15, eq. 16], [32, eq. 3.18], and [30, eq. 3.381.4] respectively.

□

REFERENCES

- [1] J. H. Winters, "Optimum combining in digital mobile radio with cochannel interference," *IEEE J. Select. Areas Commun.*, vol. SAC-2, no. 4, pp. 528–539, July 1984.
- [2] A. Shah and A. M. Haimovich, "Performance analysis of optimum combining in wireless communications with Rayleigh fading and cochannel interference," *IEEE Trans. Commun.*, vol. 46, no. 4, pp. 473–479, Oct. 1998.
- [3] V. A. Aalo and J. Zhang, "Performance of antenna array systems with optimum combining in a Rayleigh fading environment," *IEEE Commun. Lett.*, vol. 4, no. 12, pp. 387–389, Dec. 2000.
- [4] M. Chiani, M. Win, A. Zanella, J. H. Winters, "An analytical framework for the performance evaluation of optimum combining for M-PSK signals," in *Proc. 36-th Conf. on Information Science and Systems (CISS 2002)*, Princeton, NJ, 20–22 March 2002.
- [5] J. S. Kwak and J. H. Lee, "Performance analysis of optimum combining for dual-antenna diversity with multiple interferers in a Rayleigh fading channel," *IEEE Commun. Lett.*, vol. 6, no. 12, pp. 541–543, Dec. 2002.
- [6] J. S. Kwak and J. H. Lee, "Approximate error probability of M-ary PSK for optimum combining with arbitrary numbers of interferers in a Rayleigh fading channel," *IEICE Trans. Comm.*, vol. E86-B, no. 12, pp. 3544–3550, Dec. 2003.
- [7] M. Chiani, M. Z. Win, A. Zanella, R. K. Mallik, and J. H. Winters, "Bounds and approximations for optimum combining of signals in the presence of multiple co-channel interferers and thermal noise," *IEEE Trans. on Commun.*, vol. 51, no. 2, pp. 296–307, Feb. 2003.
- [8] H. Gao, P. J. Smith, and M. V. Clark, "Theoretical reliability of MMSE linear diversity combining in Rayleigh-fading additive interference channels," *IEEE Trans. on Commun.*, vol. 46, no. 5, pp. 666–672, May 1998.
- [9] M. Kang, L. Yang, and M.-S. Alouini, "Performance analysis of MIMO systems in presence of co-channel interference and additive Gaussian noise," in *Proc. 37th Annual Conf. on Info. Sciences and Systems (CISS)*, Baltimore, MD, Mar. 2003.

- [10] D. Yue, X. Wang, and F. Xu, "Performance analysis for optimum combining of Rayleigh fading signals with correlated Rayleigh interferers and noise," *IEEE Signal Processing Letters*, vol. 13, no. 5, pp. 269–272, May 2006.
- [11] M. Chiani, M. Z. Win, A. Zanella, and J. H. Winters, "Error probability for optimum combining of M -ary PSK signals in the presence of interference and noise," *IEEE Trans. Commun.*, vol. 51, no. 11, pp. 1949–1957, Nov. 2003.
- [12] D. Lao and A. M. Haimovich, "Exact closed-form performance analysis of optimum combining with multiple cochannel interferers and Rayleigh fading," *IEEE Trans. Commun.*, vol. 51, no. 6, pp. 995–1003, June 2003.
- [13] R. K. Mallik, M. Z. Win, M. Chiani, and A. Zanella, "Bit-error probability for optimum combining of binary signals in the presence of interference and noise," *IEEE Trans. Wireless Commun.*, vol. 3, no. 2, pp. 395–407, Mar. 2004.
- [14] Q. T. Zhang and X. W. Cui, "Outage probability for optimum combining of arbitrarily faded signals in the presence of correlated Rayleigh interferers," *IEEE Trans. on Veh. Technol.*, vol. 53, no. 4, pp. 1043–1051, July 2004.
- [15] A. Zanella, M. Chiani, and M. Z. Win, "MMSE reception and successive interference cancellation for MIMO systems with high spectral efficiency," *IEEE Trans. Wireless Commun.*, vol. 4, no. 3, pp. 1244–1253, May 2005.
- [16] M. Chiani, M. Z. Win, and A. Zanella, "On optimum combining of M-PSK signals with unequal-power interferers and noise," *IEEE Trans. Commun.*, vol. 53, no. 1, pp. 44–47, Jan. 2005.
- [17] D.-W. Yue, Q. T. Zhang, and C. X. Wei, "Characteristic functions for optimum combining output SINR with AWGN and correlated interference," *IEEE Trans. Commun.*, vol. 55, no. 2, pp. 266–270, Mar. 2007.
- [18] C. Chayawan and V. A. Aalo, "On the outage probability of optimum combining and maximal ratio combining schemes in an interference-limited Rice fading channel," *IEEE Trans. Commun.*, vol. 50, no. 4, pp. 532–535, Apr. 2002.
- [19] A. Shah and A. M. Haimovich, "Performance analysis of maximum ratio combining and comparison with optimum combining for mobile radio communications with cochannel interference," *IEEE Trans. Veh. Technol.*, vol. 49, no. 4, pp. 1454–1463, July 2000.
- [20] M. Kang, M.-S. Alouini, and L. Yang, "Outage probability and spectrum efficiency of cellular mobile radio systems with smart antennas," *IEEE Trans. Commun.*, vol. 50, no. 12, pp. 1871–1877, Dec. 2002.
- [21] A. T. James, "Distributions of matrix variates and latent roots derived from normal samples," *Ann. Math. Statist.*, vol. 35, pp. 475–501, 1964.
- [22] M. K. Simon and M.-S. Alouini, *Digital Communication over Fading Channels: A Unified Approach to Performance Analysis*. New York, NY: John Wiley and Sons, Inc., 2000.
- [23] M. Chiani, D. Dardari, and M. K. Simon, "New exponential bounds and approximations for the computation of error probability in fading channels," *IEEE Trans. on Wireless Comm.*, vol. 2, no. 4, pp. 840–845, July 2003.
- [24] M. Abramowitz and I. A. Stegun, *Handbook of Mathematical Functions with Formulas, Graphs, and Mathematical Tables*, 9th ed. New York: Dover Publications, 1970.
- [25] H. Bolcskei, M. Borgmann, A.J. Paulraj, "Impact of the propagation environment on the performance of space-frequency coded MIMO-OFDM," *IEEE Journal on Selected Areas in Communications*, vol. 21, no. 3, pp. 427–439, Apr. 2003.
- [26] M. Schwartz, W. R. Bennett, and S. Stein, *Communication Systems and Techniques*, New York: McGraw-Hill, 1996.
- [27] M. Chiani, M. Z. Win, and H. Shin, "A general result on hypergeometric functions of matrix arguments and application to wireless MIMO communication," in *Proc. First Int. Conf. on Next-Gen. Wireless Sys. (ICNEWS'06)*, Dhaka, Bangladesh, Jan. 2006, pp. 196–200.
- [28] M. R. McKay, A. J. Grant, and I. B. Collings, "Performance analysis of MIMO-MRC in double-correlated Rayleigh environments," *IEEE Trans. Commun.*, vol. 55, no. 3, pp. 497–507, Mar. 2007.

- [29] M. Chiani, M. Z. Win, and A. Zanella, "On the capacity of spatially correlated MIMO Rayleigh fading channels," *IEEE Trans. on Inform. Theory*, vol. 49, no. 10, pp. 2363-2371, Oct. 2003.
- [30] I. S. Gradshteyn and I. M. Ryzhik, *Tables of Integrals, Series, and Products*, 4th ed. San Diego, CA: Academic Press, Inc., 1965.
- [31] S. Jin, M. R. McKay, X. Gao, and I. B. Collings, "MIMO multichannel beamforming: SER and outage using new eigenvalue distributions of complex noncentral Wishart matrices," *IEEE Trans. Commun.*, to appear, 2007.
- [32] P. J. Smith and L. M. Garth, "Distribution and characteristic functions for correlated complex Wishart matrices," *J. Multivariate Analysis*, 2005, submitted for publication.

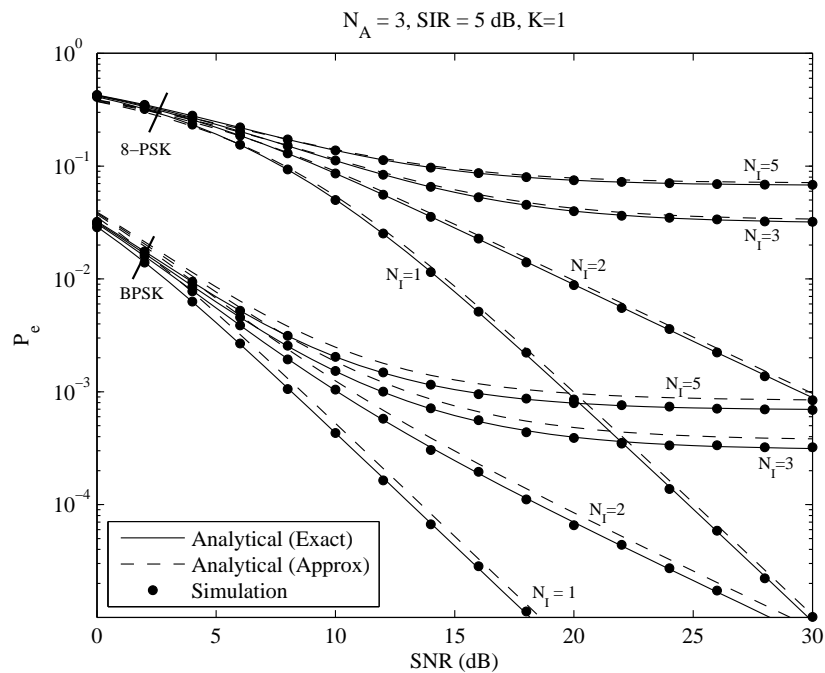


Fig. 1. SEP of Rician-Rayleigh OC as a function of SNR for $N_A = 3$, $SIR = 5$ dB, and $K = 1$; comparison between analytical and simulation results for different modulation schemes and different N_r .

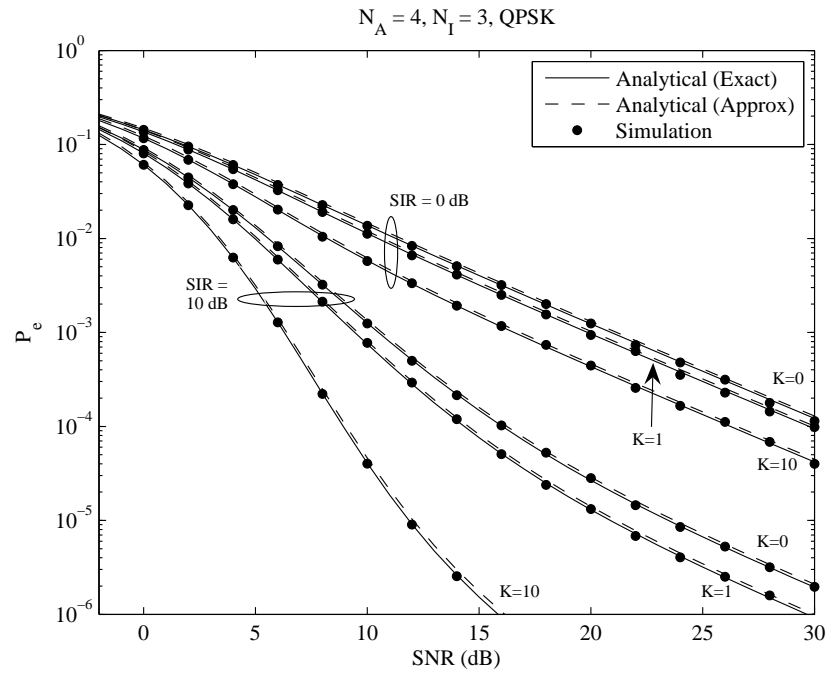


Fig. 2. SEP of Rician-Rayleigh OC as a function of SNR for $N_A = 4$, $N_I = 3$, and QPSK; analytical and simulation results for different K and different SIRs.

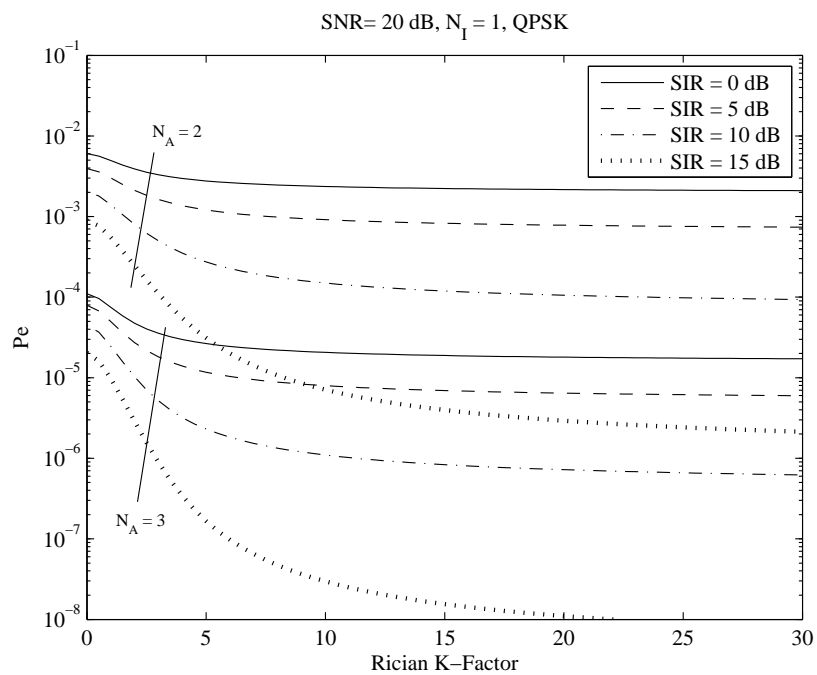


Fig. 3. SEP of Rician-Rayleigh OC as a function of K for $N_I = 1$, SNR = 20 dB, and QPSK; analytical results for different SIRs and different N_A .

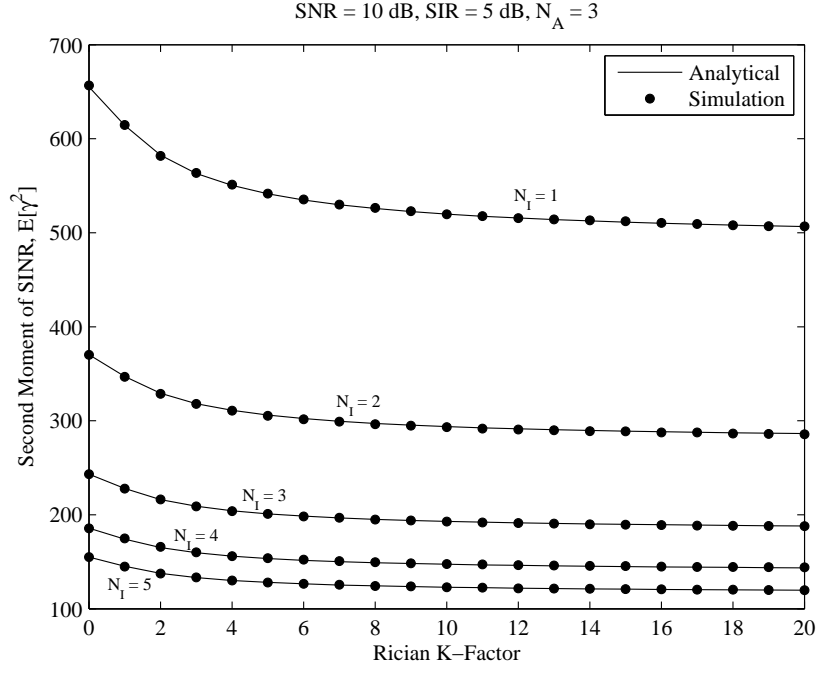


Fig. 4. Second moment of the SINR of Rician-Rayleigh OC as a function of K for $N_A = 3$, SNR = 10 dB, SIR = 5 dB; analytical and simulation results for different N_I .

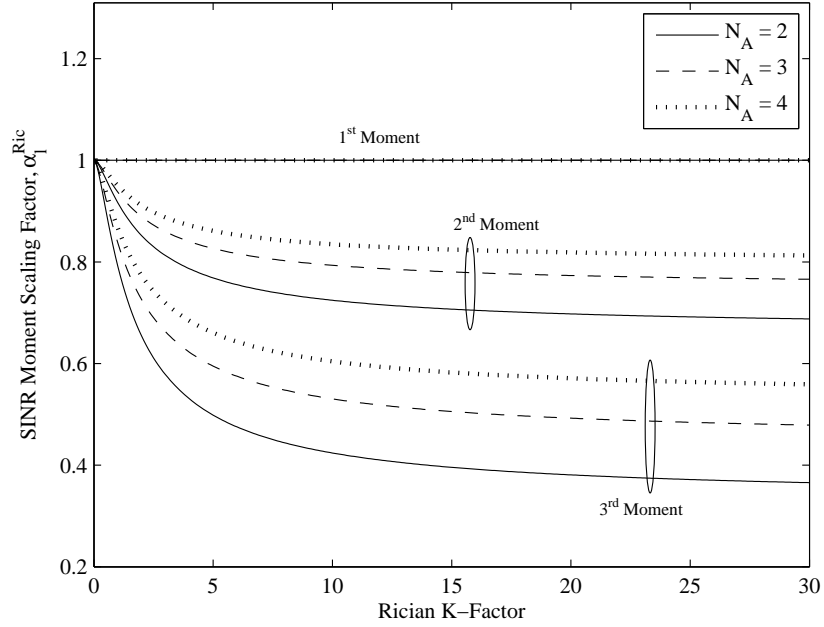


Fig. 5. Plot of α_ℓ^{Ric} as a function of K ; analytical results for different ℓ and N_A .

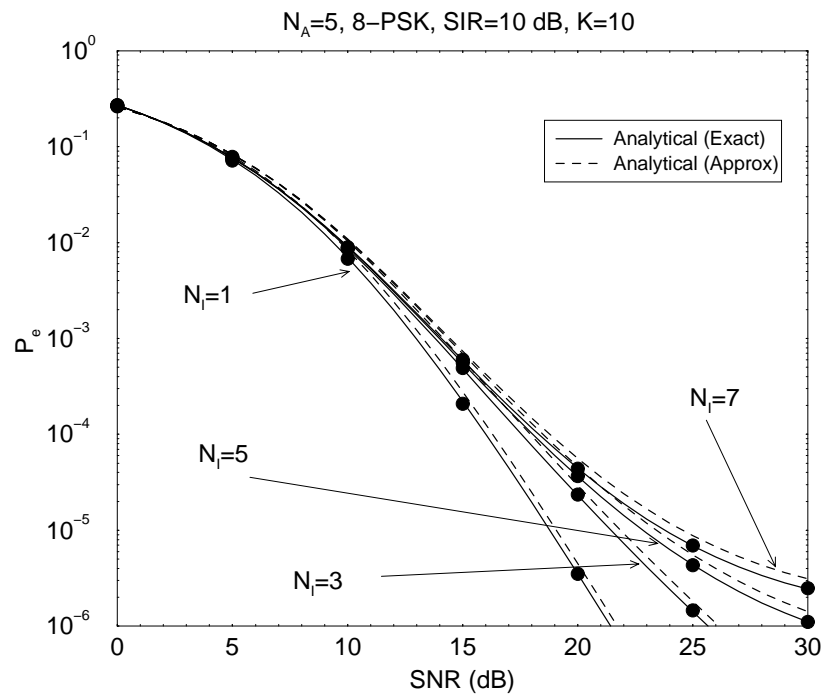


Fig. 6. SEP of Rayleigh-Rician OC as a function of SNR for $N_A = 5$, SIR = 10 dB, 8-PSK, and $K = 10$; comparison between analytical and simulation results for different N_I .

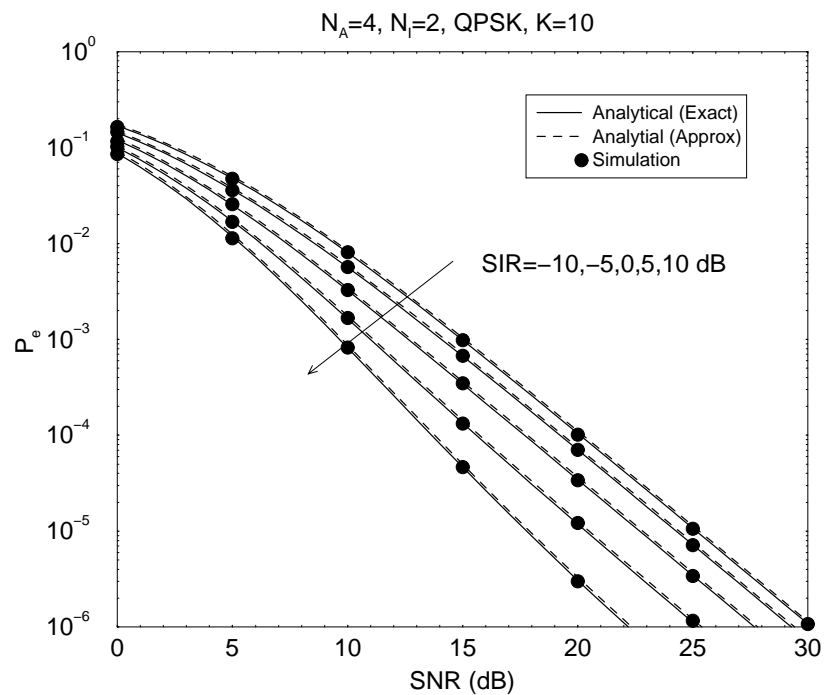


Fig. 7. SEP of Rayleigh-Rician OC as a function of SNR for $N_A = 4$, $N_I = 2$, QPSK, and $K = 10$; comparison between analytical and simulation results for different SIRs.

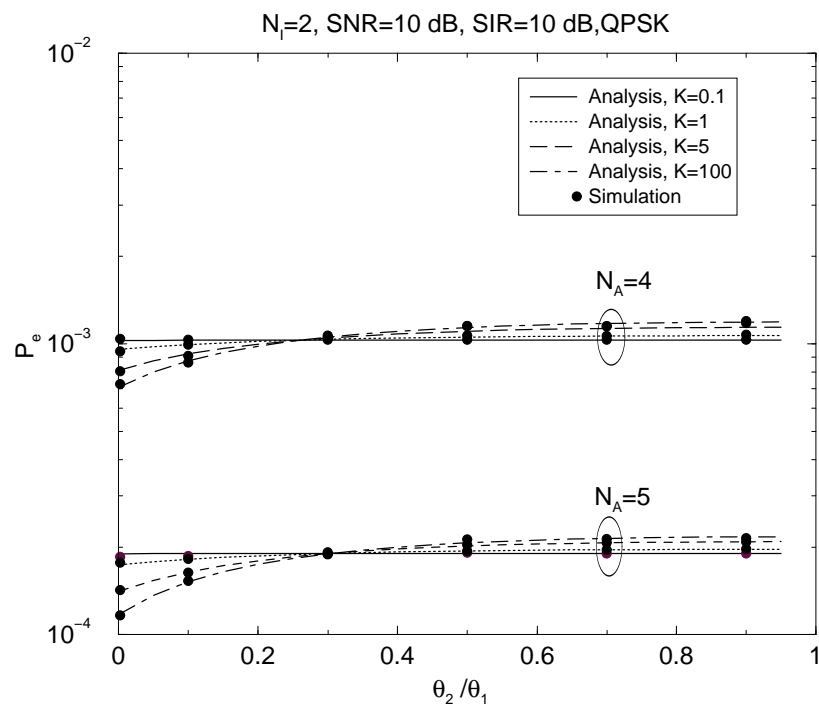


Fig. 8. SEP of Rayleigh-Rician OC as a function of the ratio θ_2/θ_1 for $N_I = 2$, SNR = 10 dB, SIR = 10 dB, and QPSK; analytical results for different N_A and different K .